
DIRICHLET PROCESS MIXTURE MODELS WITH SHRINKAGE PRIOR

A PREPRINT

Dawei Ding

Department of Mathematics, Statistics, and Computer Science
University of Illinois at Chicago
Chicago, IL 60015
dding20@uic.edu

George Karabatsos

Department of Educational Psychology,
with affiliation to the Department of Mathematics, Statistics, and Computer Science
University of Illinois at Chicago
Chicago, IL 60015
gkarabatsos1@gmail.com

ABSTRACT

We propose Dirichlet Process Mixture (DPM) models for prediction and cluster-wise variable selection, based on two choices of shrinkage baseline prior distributions for the linear regression coefficients, namely the Horseshoe prior and Normal-Gamma prior. We show in a simulation study that each of the two proposed DPM models tend to outperform the standard DPM model based on the non-shrinkage normal prior, in terms of predictive, variable selection, and clustering accuracy. This is especially true for the Horseshoe model, and when the number of covariates exceeds the within-cluster sample size. A real data set is analyzed to illustrate the proposed modeling methodology, where both proposed DPM models again attained better predictive accuracy.

Keywords Bayesian nonparametrics · Shrinkage Prior · Regression · Variable selection

1 Introduction

For linear regression with variable (covariate) selection, the LASSO provides a prominent method with many extensions (Tibshirani, 1996, 2011). This method employs a shrinkage parameter which can shrink the regression coefficients of irrelevant covariates to zero, and the corresponding LASSO estimate can be interpreted as the Bayes posterior mode under independent zero-mean Laplace prior distributions on the regression coefficients. Park and Casella (2008) first considered a fully Bayesian LASSO by exploiting the representation of the Laplace prior as a scale mixture of zero-mean normal distributions with exponential mixing density (Andrews and Mallows, 1974). However, such a choice of prior does not provide adaptive shrinkage, but instead shrinks all coefficients towards zero. Other shrinkage priors, defined by other mixing distributions, were proposed mainly to address this issue. Carvalho et al. (2009, 2010) proposed the Horseshoe prior, defined by a half-Cauchy mixing distribution, with local shrinkage parameters which help achieve robustness in handling sparsity. Griffin and Brown (2010) proposed the Normal-Gamma shrinkage prior, defined by a Gamma mixing distribution which provides adaptive tail thickness and shrinkage. These previous studies showed that, for normal linear models, models assigned the Horseshoe or Normal-Gamma prior on the coefficients tend to outperform models assigned a Laplace (LASSO) or non-shrinkage normal prior on the coefficients, in terms of parameter estimation and variable selection accuracy, especially when the number of covariates exceeds the sample size. Furthermore, statistical estimation with models based on continuous shrinkage priors, such as the Horseshoe, Normal-Gamma, and Laplace (LASSO), can be more computationally efficient than estimation with models based on

spike-and-slab priors, because the latter models can require high computational cost to search through a large number of possible submodels when there are many covariates (Castillo et al., 2015).

One key limitation of the existing shrinkage priors is that they do not allow variable selection to vary over different clusters of the data points, based on the unknown clustering estimated from the data. However, few methods have addressed this problem; see Barcella et al. (2017) for a review. Barcella et al. (2016) proposed a covariate-dependent Dirichlet Process Mixture (DPM) model which assigns a spike-and-slab prior distribution to achieve cluster-wise variable selection for binary covariates. Quintana et al. (2015) proposed cluster-wise variable selection in a product partition model by employing binary indicator parameters on the covariate similarity function. Meanwhile, the joint DPM modeling approach, defined by DPM modeling of both covariate and conditional response distributions, can provide better predictive accuracy than DPM modeling which assumes fixed covariates. This is because the approach accounts for the distance between a new covariate profile \mathbf{x} and the data-observed \mathbf{x} values of the different cluster groups (Hannah et al., 2011).

To address the key limitation, we propose two joint DPM of regression models, defined by either a Horseshoe or Normal-Gamma shrinkage baseline prior on the regression coefficients. Each shrinkage DPM model is based on the Dependent Dirichlet Process (DDP), a wide and flexible class of covariate-dependent random probability measures (MacEachern, 1999; Quintana et al., 2020). Next, in Section 2, we further describe our proposed DPM models. It also characterizes the parameter posterior distributions and conditional posterior predictive distributions, and provides corresponding MCMC sampling algorithms for the models. This section also reviews methods for summarizing the MCMC posterior sample output for variable selection and clustering estimation. In Section 3, we compare our DPM models against the standard DPM model which assigns non-shrinkage normal baseline prior on the regression coefficients, in terms of predictive, variable selection, and clustering accuracy. Section 4 illustrates our shrinkage DPM models on a real data set. Section 5 concludes the article.

2 Model and Posterior Inference

Given a data set matrix $(\mathbf{y}, \mathbf{X}) = (y_i, \mathbf{x}_i)_{i=1}^n$ including n observations of $p \times 1$ covariate vectors $\mathbf{x}_i \in \mathbb{R}^p$ and scalar responses $y_i \in \mathbb{R}$, our DPM model is the mixture of Normal (\mathcal{N}) probability densities:

$$(y_i, \mathbf{x}_i) | G, \sigma^2 \stackrel{iid}{\sim} \int \mathcal{N}(y | \mu + \mathbf{x}^T \boldsymbol{\beta}, \sigma^2) \mathcal{N}_p(\mathbf{x} | \mathbf{m}, \text{diag}(\boldsymbol{\tau})) G(d\boldsymbol{\theta}), \quad (1)$$

for $i = 1, \dots, n$, where $\boldsymbol{\theta} = \{\boldsymbol{\theta}_y, \boldsymbol{\theta}_x\}$, $\boldsymbol{\theta}_y = \{\mu, \boldsymbol{\beta}\}$, $\boldsymbol{\theta}_x = \{\mathbf{m}, \boldsymbol{\tau}\}$, $\boldsymbol{\beta} = (\beta_1, \dots, \beta_p)$, $\mathbf{m} = (m_1, \dots, m_p)$, and $\boldsymbol{\tau} = (\tau_1, \dots, \tau_p)$ with mixing distribution $G \sim \text{DP}(\alpha, G_0)$ assigned a Dirichlet Process prior with mass parameter $\alpha > 0$ and baseline measure G_0 (Ferguson, 1973).

Since the support of the DP prior is almost surely discrete, the general mixture model (1) can also be expressed as the countable mixture:

$$f(y, \mathbf{x} | G, \sigma^2) = \sum_{j=1}^{\infty} \mathcal{N}(y | \mu_j + \mathbf{x}^T \boldsymbol{\beta}_j, \sigma^2) \mathcal{N}_p(\mathbf{x} | \mathbf{m}_j, \text{diag}(\boldsymbol{\tau}_j)) w_j. \quad (2)$$

The Dirichlet Process G in (1) admits the stick-breaking representation of infinite mixture $G(\cdot) = \sum_{j=1}^{\infty} w_j \delta_{\boldsymbol{\theta}_j}(\cdot)$, where

$\boldsymbol{\theta}_j = \{\mu_j, \boldsymbol{\beta}_j, \mathbf{m}_j, \boldsymbol{\tau}_j\} \stackrel{iid}{\sim} G_0$, $\delta_{\boldsymbol{\theta}_j}$ is the Dirac measure that takes the value 1 on $\boldsymbol{\theta}_j$ and 0 elsewhere, and the mixing weights have the stick-breaking form $w_j = v_j \prod_{l=1}^{j-1} (1 - v_l)$ with $v_j \stackrel{iid}{\sim} \text{Beta}(1, \alpha)$ for $j = 1, 2, \dots$, $\sum_{j=1}^{\infty} w_j = 1$ (Sethuraman, 1994).

The conditional density of Y in the joint mixture model (2) can be written as:

$$f(y | \mathbf{x}, G, \sigma^2) = \sum_{j=1}^{\infty} \mathcal{N}(y | \mu_j + \mathbf{x}^T \boldsymbol{\beta}_j, \sigma^2) w_j(\mathbf{x}),$$

with covariate dependent mixture weights $w_j(\mathbf{x}) = \frac{w_j \mathcal{N}_p(\mathbf{x} | \mathbf{m}_j, \text{diag}(\boldsymbol{\tau}_j))}{\sum_{h=1}^{\infty} w_h \mathcal{N}_p(\mathbf{x} | \mathbf{m}_h, \text{diag}(\boldsymbol{\tau}_h))}$, implying that the model is based on the Dependent Dirichlet Process (Quintana et al., 2020).

2.1 Horseshoe DPM Model (HS-DPM)

The HS-DPM model is completed by the specification of the following prior distributions, while defining the baseline measure G_0 according to the Horseshoe prior (Carvalho et al., 2010) for the regression coefficients in the infinite component representation (2):

$$g_0(\mu_j, \beta_j, \mathbf{m}_j, \boldsymbol{\tau}_j) = \mathcal{N}(\mu_j|0, \nu_\mu) \mathcal{N}_p(\beta_j|\mathbf{0}, \zeta_j^2 \sigma^2 \boldsymbol{\Gamma}_j) \prod_{l=1}^p \left[\mathcal{N}(m_{jl}|m_0, \frac{\tau_{jl}}{n_0}) IG(\tau_{jl}|\frac{\nu_0}{2}, \frac{2}{\nu_0 s_0^2}) \right] \quad (3a)$$

$$\boldsymbol{\Gamma}_j = \text{diag}(\gamma_{j1}^2, \dots, \gamma_{jp}^2) \equiv \text{diag}(\boldsymbol{\gamma}_j^2), \quad j = 1, 2, \dots \quad (3b)$$

$$\pi(\boldsymbol{\gamma}_j) = \prod_{l=1}^p \mathcal{C}^+(\gamma_{jl}|0, 1), \quad j = 1, 2, \dots \quad (3c)$$

$$\pi(\zeta_j) = \mathcal{C}^+(\zeta_j|0, 1), \quad j = 1, 2, \dots \quad (3d)$$

$$\pi(\mathbf{v}) = \prod_{j=1}^{\infty} \text{Beta}(v_j|1, \alpha) \quad (3e)$$

$$\pi(\alpha) = \text{Ga}(\alpha|\alpha_\alpha, \theta_\alpha) \quad (3f)$$

$$\pi(\sigma^2) = \text{IG}(\sigma^2|\alpha_0, \theta_0). \quad (3g)$$

Above, g_0 is the pdf of the baseline measure G_0 , $IG(c, d)$ is the Inverse-gamma distribution with shape c and scale d , $\mathcal{C}^+(0, 1)$ is the standard half-Cauchy distribution, and $\text{Ga}(c, d)$ is the Gamma distribution with shape c and rate d .

2.2 Normal-Gamma DPM Model (NG-DPM)

The NG-DPM model is completed by the specification of the following prior density functions for the model parameters, while defining the baseline measure G_0 according to the Normal-Gamma prior (Griffin and Brown, 2010) for the regression coefficients in the infinite component representation (2):

$$g_0(\mu_j, \beta_j, \mathbf{m}_j, \boldsymbol{\tau}_j) = \mathcal{N}(\mu_j|0, \nu_\mu) \mathcal{N}_p(\beta_j|\mathbf{0}, \mathbf{D}_{\psi_j}) \prod_{l=1}^p \left[\mathcal{N}(m_{jl}|m_0, \frac{\tau_{jl}}{n_0}) IG(\tau_{jl}|\frac{\nu_0}{2}, \frac{2}{\nu_0 s_0^2}) \right] \quad (4a)$$

$$\mathbf{D}_{\psi_j} = \text{diag}(\psi_{j1}, \dots, \psi_{jp}) \equiv \text{diag}(\boldsymbol{\psi}_j), \quad j = 1, 2, \dots \quad (4b)$$

$$\pi(\boldsymbol{\psi}_j|\lambda_j, \gamma_j^{-2}) = \prod_{l=1}^p \text{Ga}(\psi_{jl}|\lambda_j, \frac{1}{2}\gamma_j^{-2}), \quad j = 1, 2, \dots \quad (4c)$$

$$\pi(\lambda_j, \gamma_j^{-2}) = \text{Exp}(\lambda_j|1) \text{Ga}(\gamma_j^{-2}|2, \frac{2V}{\lambda_j}), \quad j = 1, 2, \dots \quad (4d)$$

$$\pi(\mathbf{v}) = \prod_{j=1}^{\infty} \text{Beta}(v_j|1, \alpha) \quad (4e)$$

$$\pi(\alpha) = \text{Ga}(\alpha|\alpha_\alpha, \theta_\alpha) \quad (4f)$$

$$\pi(\sigma^2) = \text{IG}(\sigma^2|\alpha_0, \theta_0), \quad (4g)$$

where $\text{Exp}(1)$ is the Exponential distribution with rate 1, $V = \frac{1}{p} \sum_{l=1}^p \hat{\beta}_l^2 \mathbf{1}(n \geq p+1) + \frac{1}{n} \sum_{l=1}^p \tilde{\beta}_l^2 \mathbf{1}(n < p+1)$, $\mathbf{1}(\cdot)$ is the indicator function, $(\hat{\boldsymbol{\mu}}, \hat{\boldsymbol{\beta}}^T)^T = (\tilde{\mathbf{X}}^T \tilde{\mathbf{X}})^{-1} \tilde{\mathbf{X}}^T \mathbf{y}$ is the least squares estimate, $(\tilde{\boldsymbol{\mu}}, \tilde{\boldsymbol{\beta}}^T)^T = \tilde{\mathbf{X}}^T (\tilde{\mathbf{X}} \tilde{\mathbf{X}}^T)^{-1} \mathbf{y}$ is the minimum norm least squares estimate, and $\tilde{\mathbf{X}} = [\mathbf{1}_n, \mathbf{X}]$.

For the HS-DPM and the NG-DPM model, the joint prior density of all the model parameters $\boldsymbol{\Lambda} = (\boldsymbol{\theta}, \sigma^2)$ in model (3) or (4) is denoted by $\pi(\boldsymbol{\Lambda})$, respectively.

2.3 Posterior Computations

In order to enable tractable posterior-based inferences, the infinite dimensionality of the HS-DPM model or NG-DPM model can be handled by the introduction of latent variables u_i and cluster membership indicators d_i for $i = 1, \dots, n$.

Then, for either model, it can be shown that the joint posterior distribution of all the model parameters Λ and $\{(u_i, d_i), i = 1, \dots, n\}$, is proportional to:

$$\prod_{i=1}^n \left[\mathbf{1}(u_i < w_{d_i}) \mathcal{N}(y_i | \mu_{d_i} + \mathbf{x}^T \boldsymbol{\beta}_{d_i}, \sigma^2) \prod_{l=1}^p \mathcal{N}(x_{il} | m_{d_i, l}, \tau_{d_i, l}) \right] \pi(\Lambda) \quad (5)$$

where $d_i = j$ if observation pair (y_i, \mathbf{x}_i) belongs to j th cluster, for $j = 1, 2, \dots$. Posterior inference of the DPM model proceeds after marginalizing over the latent variables $\{u_i : i = 1, \dots, n\}$.

Posterior inference with the HS-DPM or NG-DPM model can be undertaken by using an MCMC sampling algorithm, which embeds the Gibbs sampling algorithm for normal linear models assigned a Horseshoe prior (Makalic and Schmidt, 2015), or assigned a Normal-Gamma prior (Griffin and Brown, 2010), within a slice sampler for DPM regression models (Karabatsos and Walker, 2012). The Appendix provides more details.

2.4 Posterior Predictive Inference

Posterior-based prediction from the HS-DPM or NG-DPM model is based on a generalized Pólya urn scheme (Hannah et al., 2011; Wade et al., 2014), described as follows. A clustering of the n data points is denoted as $\rho_n = \{d_i\}_{i=1}^n$, comprised of K distinct clusters or values of the d_i . Denote the corresponding cluster sets and members as $C_j = \{i : d_i = j\}$ and $\mathbf{X}_j^* = \{\mathbf{x}_i : i \in C_j\}$, $\mathbf{y}_j^* = \{y_i : i \in C_j\}$, for $j = 1, \dots, K$. Then, based on a covariate-dependent Pólya urn scheme, the cluster label for a new subject d_{n+1} conditionally on its corresponding profile \mathbf{x} , current clustering ρ_n , and observations \mathbf{X} , has distribution given by:

$$d_{n+1} | \mathbf{x}, \mathbf{X}, \rho_n \sim \frac{\alpha \pi_n}{b_0} f_{0, \mathbf{x}}(\mathbf{x}) \delta_{K+1}(\cdot) + \frac{1}{b_0} \sum_{j=1}^K \pi_n n_j f_{j, \mathbf{x}}(\mathbf{x}) \delta_j(\cdot), \quad (6)$$

where $\pi_n = \frac{1}{\alpha + n}$, $n_j = |C_j|$, $\sum_{j=1}^K n_j = n$, $b_0 = p(\mathbf{x} | \rho_n, \mathbf{X})$,

$$f_{0, \mathbf{x}}(\mathbf{x}) = \int \mathcal{N}_p(\mathbf{x} | \boldsymbol{\theta}_{\mathbf{x}}) G_0(d\boldsymbol{\theta}_{\mathbf{x}}), \text{ and } f_{j, \mathbf{x}}(\mathbf{x}) = \int \mathcal{N}_p(\mathbf{x} | \boldsymbol{\theta}_{\mathbf{x}}) p(\boldsymbol{\theta}_{\mathbf{x}} | \mathbf{X}_j^*) d\boldsymbol{\theta}_{\mathbf{x}}.$$

Thus, the cluster allocation probability distribution (6) depends on new \mathbf{x} and the covariate data \mathbf{X} . The more similar a new profile \mathbf{x} is to the existing \mathbf{x}_i 's in cluster j , the higher the density $p(\mathbf{x} | \boldsymbol{\theta}_{\mathbf{x}})$, leading to higher predictive density $f_{j, \mathbf{x}}(\mathbf{x})$, thus the higher probability of allocation to cluster j .

Once we obtain the allocation scheme for a new subject, we can then derive the conditional predictive density of the subject's response y for fixed variance σ^2 , given her new profile \mathbf{x} and the data (\mathbf{y}, \mathbf{X}) , as:

$$\begin{aligned} f(y | \mathbf{y}, \mathbf{X}, \mathbf{x}) &= \sum_{\rho_n} \sum_{d_{n+1}} f(y | \mathbf{y}, \mathbf{X}, \mathbf{x}, \rho_n, d_{n+1}) p(d_{n+1} | \mathbf{X}, \mathbf{x}, \rho_n) p(\rho_n | \mathbf{y}, \mathbf{X}, \mathbf{x}) \\ &= \sum_{\rho_n} \left[\frac{\alpha \pi_n}{b_0} f_{0, \mathbf{x}}(\mathbf{x}) f_{0, y}(y | \mathbf{x}) + \frac{1}{b_0} \sum_{j=1}^K n_j \pi_n f_{j, \mathbf{x}}(\mathbf{x}) f_{j, y}(y | \mathbf{x}) \right] \frac{p(\mathbf{x} | \rho_n, \mathbf{X}) p(\rho_n | \mathbf{y}, \mathbf{X})}{p(\mathbf{x} | \mathbf{y}, \mathbf{X})} \\ &= \sum_{\rho_n} \left[\frac{\alpha \pi_n}{b_0} f_{0, \mathbf{x}}(\mathbf{x}) f_{0, y}(y | \mathbf{x}) + \frac{1}{b_0} \sum_{j=1}^K n_j \pi_n f_{j, \mathbf{x}}(\mathbf{x}) f_{j, y}(y | \mathbf{x}) \right] \frac{b_0 p(\rho_n | \mathbf{y}, \mathbf{X})}{p(\mathbf{x} | \mathbf{y}, \mathbf{X})} \\ &= \sum_{\rho_n} \left[\frac{\alpha \pi_n}{b} f_{0, \mathbf{x}}(\mathbf{x}) f_{0, y}(y | \mathbf{x}) + \frac{1}{b} \sum_{j=1}^K n_j \pi_n f_{j, \mathbf{x}}(\mathbf{x}) f_{j, y}(y | \mathbf{x}) \right] p(\rho_n | \mathbf{y}, \mathbf{X}) \\ &= \sum_{\rho_n} f(y | \mathbf{y}, \mathbf{X}, \mathbf{x}, \rho_n) p(\rho_n | \mathbf{y}, \mathbf{X}), \end{aligned}$$

where $p(\rho_n | \mathbf{y}, \mathbf{X})$ is the posterior of the clustering ρ_n on n observations,

$$b = p(\mathbf{x} | \mathbf{y}, \mathbf{X}), \quad f_{0, y}(y | \mathbf{x}) = \int \mathcal{N}(y | \mathbf{x}, \boldsymbol{\theta}_y) G_0(d\boldsymbol{\theta}_y), \text{ and } f_{j, y}(y | \mathbf{x}) = \int \mathcal{N}(y | \mathbf{x}, \boldsymbol{\theta}_y) p(\boldsymbol{\theta}_y | \mathbf{y}_j^*, \mathbf{X}_j^*) d\boldsymbol{\theta}_y.$$

Thus, given each partition (clustering) of the data, the conditional posterior predictive density is a weighted average of the conditional predictive density with parameters drawn from baseline distribution and the cluster-wise conditional

predictive density. In practice, the conditional predictive density can be approximated by averaging over S MCMC posterior samples of ρ_n , using:

$$f(y|\mathbf{y}, \mathbf{X}, \mathbf{x}) \approx \frac{1}{S} \sum_{s=1}^S \hat{f}^{(s)}(y|\mathbf{y}, \mathbf{X}, \mathbf{x}, \rho_n^{(s)}).$$

Based on the same covariate-dependent urn scheme structure, the posterior predictive expectation, conditionally on a new \mathbf{x} , is given by:

$$E(Y|\mathbf{y}, \mathbf{X}, \mathbf{x}) = \sum_{\rho_n} \left[\frac{\alpha \pi_n}{b} f_{0,\mathbf{x}}(\mathbf{x}) E_0(Y|\mathbf{x}) + \frac{1}{b} \sum_{j=1}^K n_j \pi_n f_{j,\mathbf{x}}(\mathbf{x}) E_j(Y|\mathbf{x}) \right] p(\rho_n|\mathbf{y}, \mathbf{X}),$$

where $E_0(Y|\mathbf{x})$ is the expectation of y given \mathbf{x} with distribution $f_{0,y}(y|\mathbf{x})$ and $E_j(Y|\mathbf{x})$ is the expectation of Y given \mathbf{x} with distribution $f_{j,y}(y|\mathbf{x})$. The predictive expectation can be approximated by averaging over MCMC posterior samples of ρ_n , i.e.,

$$E(Y|\mathbf{y}, \mathbf{X}, \mathbf{x}) \approx \frac{1}{S} \sum_{s=1}^S \hat{E}(Y|\mathbf{x}, \boldsymbol{\theta}_{1:n}^{(s)}),$$

where:

$$E(Y|\mathbf{x}, \boldsymbol{\theta}_{1:n}) = \frac{1}{b} \left[\alpha \int (\mu + \mathbf{x}^T \boldsymbol{\beta}) \prod_{l=1}^p \mathcal{N}(x_l|m_l, \tau_l) G_0(d\boldsymbol{\theta}) + \sum_{j=1}^n (\mu_{d_j} + \mathbf{x}^T \boldsymbol{\beta}_{d_j}) \prod_{l=1}^p \mathcal{N}(x_l|m_{d_j,l}, \tau_{d_j,l}) \right],$$

$$\text{and } b = \alpha \int \prod_{l=1}^p \mathcal{N}(x_l|m_l, \tau_l) G_0(d\boldsymbol{\theta}) + \sum_{i=1}^n \prod_{l=1}^p \mathcal{N}(x_l|m_{d_i,l}, \tau_{d_i,l}).$$

2.5 Variable Selection

The regression coefficients β 's do not have positive probabilities of taking on a value of zero in the prior or the posterior, due to the absolute continuity of the Horseshoe or Normal-Gamma shrinkage prior. However, it is possible to adopt the Scaled Neighborhood (SN) criterion of Li and Lin (2010) for variable selection. Specifically, for each data point and its estimated posterior cluster membership \hat{d}_i for $i = 1, \dots, n$ obtained by an optimal clustering rule (see Section 2.6), we obtain the MCMC posterior samples of coefficients matrix $\mathbf{B}_{\hat{d}_i} = (\boldsymbol{\beta}_{\hat{d}_i,1}, \dots, \boldsymbol{\beta}_{\hat{d}_i,p})$, where $\boldsymbol{\beta}_{\hat{d}_i,l}$ (for $l = 1, \dots, p$) are S -dimensional vectors consisting of posterior samples. Then, for each $l = 1, \dots, p$, we compute the coordinate-wise (SN) posterior probability P_{il} that β_l is within the scaled neighborhood $[-\sqrt{\text{var}(\beta_{\hat{d}_i,l}|\mathbf{y}, \mathbf{X})}, \sqrt{\text{var}(\beta_{\hat{d}_i,l}|\mathbf{y}, \mathbf{X})}]$, based on marginal posterior variances estimated from the MCMC sampling algorithm. Then the decision of whether to exclude the l th covariate for observation i in cluster \hat{d}_i depends on whether the SN probability P_{il} exceeds a threshold p^* , usually chosen as $p^* = \frac{1}{2}$.

2.6 Clustering

In Bayesian inference, an optimal point estimator $\hat{\rho}$ of the clustering is obtained by the minimizing solution:

$$\hat{\rho} = \arg \min_{\rho'} \sum_{\rho_n} \mathcal{L}(\rho', \rho_n) p(\rho_n|\mathbf{y}, \mathbf{X}),$$

where \mathcal{L} is a chosen loss function. Here, we choose the loss function $\mathcal{L}(a, z)$ by the variation of information (VI) (Meilă, 2007), which is based on information theory and is invariant to label-switching of the cluster assignments $\rho_n = \{d_i\}_{i=1}^n$. The VI between two clusterings (ρ', ρ_n) is the sum of their Shannon entropies minus twice the information they share. For clustering estimation we implemented the greedy algorithm of Rastelli and Friel (2018), which aims to

find the minimizing solution $\hat{\rho} = \arg \min_{\rho'} \frac{1}{S} \sum_{s=1}^S \mathcal{L}(\rho', \rho_{n,s})$, based on S MCMC posterior samples of the clusterings $\rho_{n,s} = \{d_{i,s}\}_{i=1}^n \sim \pi(\rho_n|\mathbf{y}, \mathbf{X})$ for $s = 1, \dots, S$.

According to the random partition characteristic of the joint DPM model, under moderate or high number of covariates p , the likelihood for covariates tends to dominate the posterior of the clustering. This could lead to a clustering that is mainly determined by covariate information, resulting more clusters with only few observations within each cluster

when the true covariate distribution is closer to the uniform distribution on a cube (Wade et al., 2014). To alleviate this potential issue and improve clustering estimation, we specify the prior parameter of DP mass parameter α as $\alpha_\alpha = 2$ and $\theta_\alpha = 20$ for the real data set analyzed in Sections 4, in order to enforce the prior expected number of clusters conditional on α is given by $E[\text{number of distinct } d'_i s] = \sum_{i=1}^n \frac{\alpha}{\alpha+i-1}$ (Escobar, 1994), so that smaller α corresponds to a smaller number of clusters on average.

3 Simulation Study

We compare the HS-DPM model, NG-DPM model, with N-DPM model as our benchmark model, in terms of prediction, variable selection, and clustering accuracy, over 10 dataset replications of various data simulation conditions, differing by sample size ($n = 100, 200, \text{ or } 400$), covariate dimensionality ($p = 10, 50, 100, 200, \text{ or } 300$), and number of components ($J = 4 \text{ or } 10$). The N-DPM model is the standard DPM model assigned a normal baseline prior distribution which enforces non-shrinkage variable selection, defined by:

$$g_0(\mu_j, \beta_j, \mathbf{m}_j, \tau_j) = \mathcal{N}_{p+1}((\mu_j, \beta_j) | \boldsymbol{\eta}, \boldsymbol{\Sigma}) \prod_{l=1}^p \left[\mathcal{N}(m_{jl} | m_0, \frac{\tau_{jl}}{n_0}) IG(\tau_{jl} | \frac{\nu_0}{2}, \frac{2}{\nu_0 s_0^2}) \right],$$

with hyperpriors $\boldsymbol{\eta} \sim \mathcal{N}_{p+1}(\mathbf{0}, 100 \cdot \mathbf{I}_{p+1})$ and $\boldsymbol{\Sigma}^{-1} \sim \text{Wishart}(p+1, 10 \cdot \mathbf{I}_{p+1})$. Throughout the simulations, all models are assumed the same hyperparameter prior specifications as $n_0 = 0.1, m_0 = 0, \nu_0 = 2, s_0^2 = 2, \alpha_0 = 2, \theta_0 = 2$, and $\alpha_\alpha = 2, \theta_\alpha = 2$. Data sets were simulated based on a mixture of J -component normal mixture for (y, \mathbf{x}) , with equal mixture weights $1/J$, as follows. Each data set was simulated by sampling each data point (y_i, \mathbf{x}_i) from $d_i \sim \text{DiscreteUniform}(1, J)$, $x_{il} \sim \mathcal{N}(m_{d_i, l}, \tau_{d_i, l})$ for $l = 1, \dots, p$, and $y_i \sim \mathcal{N}(\mu_{d_i} + \mathbf{x}_i^T \beta_{d_i}, \sigma^2)$ for $i = 1, \dots, n$. For $j = 1, \dots, J$, $\boldsymbol{\tau}_j \equiv (1, \dots, 1)^T$, $\mathbf{m}_j = j \times (2, \dots, 2)^T$, $\mu_j = [10 - 2 \times (j-1)] \mathbf{1}(j \leq 5) + [10 - 2j] \mathbf{1}(j > 5)$, $\beta_j = (\underbrace{3, \dots, 3}_{6-j}, 0, \dots, 0)^T$ if $j \leq 5$ else $\beta_j = (\underbrace{-3, \dots, -3}_{j-5}, 0, \dots, 0)^T$, with error variance $\sigma^2 = 1$. For each

simulated data set analyzed, the models are fitted using 5,000 MCMC sampling iterations, which reliably produced samples that converged to the posterior distribution according to univariate trace plots, after excluding the 2,000 initial samples as burn-in.

We compared the HS-DPM, NG-DPM, and N-DPM models according to the following criteria:

- **Prediction accuracy:** This was measured by $L1 = \frac{1}{n_t} \sum_{i=1}^{n_t} |y_{n+i} - E[Y_{n+i} | \mathbf{x}_{n+i}]|$ and $L2 = \frac{1}{n_t} \sum_{i=1}^{n_t} (y_{n+i} - E[Y_{n+i} | \mathbf{x}_{n+i}])^2$ predictive error on stand-alone test data of size $n_t = 100$, simulated as above.
- **Variable selection accuracy:** This is evaluated using Average Area Under the Curve scores $\text{A-AUC} = \frac{1}{n} \sum_{i=1}^n \text{AUC}_i$ based on Receiver Operation Characteristic curve analysis. Here AUC_i is computed according to observation i 's corresponding coefficient posterior probability P_{il} (the SN probability; see Section 2.5) against its true relevant predictor label $\mathbf{1}(\beta_{d_i, l} \neq 0)$ for $l = 1, \dots, p$, where β_{d_i} is the true regression coefficient in the cluster group d_i that sampled data point (y_i, \mathbf{x}_i) belongs to. The parameter estimation performances are also measured by Average Squared Error $\text{ASE} = \frac{1}{n} \sum_{i=1}^n \frac{1}{p} \|\hat{\beta}_{\hat{d}_i}^{\text{med}} - \beta_{d_i}\|^2$, where \hat{d}_i is the i 's cluster membership index from estimated optimal clustering rule $\hat{\rho} = \{\hat{d}_1, \dots, \hat{d}_n\}$ (Section 2.6), and $\hat{\beta}_{\hat{d}_i}^{\text{med}}$ is the posterior median of slope coefficients based on the estimated cluster group \hat{d}_i .
- **Clustering accuracy:** Clustering performance is evaluated by the the Adjusted Rand Index (Hubert and Arabie, 1985), and the estimated number of clusters, \hat{J} , obtained from the method in Section 2.6.

Condition			$L1$			$L2$		
n	p	J	HS	NG	N	HS	NG	N
100	100	4	0.98 (0.10)	2.54 (0.39)	13.86 (2.46)	1.57 (0.33)	11.75 (3.77)	314.31 (111.08)
100	200	4	0.95 (0.15)	3.79 (0.58)	56.25 (7.09)	1.43 (0.44)	23.53 (6.57)	4962.52 (1108.27)
200	10	4	0.96 (0.26)	0.96 (0.25)	0.98 (0.22)	2.68 (3.91)	2.65 (3.73)	2.54 (3.32)
200	50	4	0.93 (0.13)	0.96 (0.15)	1.75 (0.25)	1.35 (0.39)	1.46 (0.44)	4.91 (1.55)
200	100	4	0.95 (0.13)	1.12 (0.14)	2.69 (0.24)	1.43 (0.32)	1.85 (0.44)	11.35 (1.76)
200	200	4	0.93 (0.13)	1.33 (0.40)	23.81 (4.78)	1.34 (0.40)	3.67 (3.22)	911.31 (399.75)
200	300	4	1.27 (0.13)	2.02 (0.30)	64.22 (6.91)	3.45 (1.02)	8.09 (2.62)	6682.93 (1428.73)
200	50	10	1.64 (0.48)	2.57 (0.91)	4.48 (1.77)	6.89 (4.11)	18.16 (17.67)	48.01 (45.05)
200	100	10	1.55 (0.15)	3.60 (1.09)	8.13 (2.01)	4.61 (0.95)	28.06 (20.87)	113.87 (53.20)
200	200	10	2.48 (0.33)	5.99 (1.11)	31.52 (6.06)	11.55 (4.21)	67.13 (25.35)	1636.01 (623.85)
400	50	4	0.80 (0.05)	0.83 (0.06)	1.08 (0.06)	1.02 (0.12)	1.07 (0.11)	1.78 (0.20)
400	100	4	0.87 (0.08)	0.98 (0.07)	1.76 (0.18)	1.22 (0.17)	1.51 (0.19)	4.99 (0.93)
400	200	4	0.88 (0.13)	1.03 (0.13)	2.75 (0.35)	1.24 (0.32)	1.64 (0.39)	11.52 (2.76)
400	50	10	0.94 (0.16)	1.33 (0.46)	3.00 (1.11)	1.64 (0.94)	4.33 (4.12)	17.39 (12.52)
400	100	10	1.27 (0.29)	1.59 (0.43)	4.74 (1.45)	3.09 (1.67)	4.90 (2.68)	53.81 (54.54)
Condition			ARI			\hat{J}		
n	p	J	HS	NG	N	HS	NG	N
100	100	4	1.00 (0.00)	1.00 (0.00)	1.00 (0.00)	4.00 (0.00)	4.00 (0.00)	4.00 (0.00)
100	200	4	1.00 (0.00)	1.00 (0.00)	1.00 (0.00)	4.00 (0.00)	4.00 (0.00)	4.00 (0.00)
200	10	4	1.00 (0.00)	1.00 (0.00)	1.00 (0.00)	4.00 (0.00)	4.00 (0.00)	4.00 (0.00)
200	50	4	1.00 (0.00)	1.00 (0.00)	1.00 (0.00)	4.00 (0.00)	4.00 (0.00)	4.00 (0.00)
200	100	4	1.00 (0.00)	1.00 (0.00)	1.00 (0.00)	4.00 (0.00)	4.00 (0.00)	4.00 (0.00)
200	200	4	1.00 (0.00)	1.00 (0.00)	1.00 (0.00)	4.00 (0.00)	4.00 (0.00)	4.00 (0.00)
200	300	4	1.00 (0.00)	0.90 (0.06)	0.96 (0.05)	4.00 (0.00)	3.67 (0.47)	3.86 (0.35)
200	50	10	0.92 (0.01)	0.89 (0.02)	0.93 (0.02)	9.29 (0.45)	8.89 (0.99)	9.30 (0.78)
200	100	10	0.92 (0.01)	0.90 (0.01)	0.86 (0.02)	9.25 (0.43)	9.10 (0.70)	8.60 (0.92)
200	200	10	0.78 (0.01)	0.80 (0.02)	0.73 (0.03)	7.67 (0.47)	8.00 (1.05)	7.30 (1.10)
400	50	4	1.00 (0.00)	1.00 (0.00)	1.00 (0.00)	4.00 (0.00)	4.00 (0.00)	4.00 (0.00)
400	100	4	1.00 (0.00)	1.00 (0.00)	1.00 (0.00)	4.00 (0.00)	4.00 (0.00)	4.00 (0.00)
400	200	4	1.00 (0.00)	1.00 (0.00)	1.00 (0.00)	4.00 (0.00)	4.00 (0.00)	4.00 (0.00)
400	50	10	0.98 (0.01)	0.88 (0.02)	0.93 (0.01)	9.75 (0.43)	8.86 (0.99)	9.30 (0.46)
400	100	10	0.92 (0.02)	0.88 (0.02)	0.89 (0.02)	9.12 (0.78)	8.70 (0.78)	8.90 (0.83)
Condition			ASE			A-AUC		
n	p	J	HS	NG	N	HS	NG	N
100	100	4	0.00 (0.00)	0.13 (0.05)	3.33 (1.12)	1.00 (0.00)	0.99 (0.01)	0.76 (0.13)
100	200	4	0.00 (0.00)	0.12 (0.01)	26.39 (2.54)	1.00 (0.00)	0.94 (0.04)	0.49 (0.20)
200	10	4	0.02 (0.00)	0.02 (0.01)	0.02 (0.01)	1.00 (0.00)	1.00 (0.00)	1.00 (0.00)
200	50	4	0.00 (0.00)	0.01 (0.00)	0.08 (0.02)	0.88 (0.03)	0.90 (0.03)	0.92 (0.04)
200	100	4	0.00 (0.00)	0.00 (0.00)	0.10 (0.01)	0.89 (0.04)	0.89 (0.03)	0.99 (0.01)
200	200	4	0.00 (0.00)	0.01 (0.01)	4.43 (1.72)	1.00 (0.00)	1.00 (0.00)	0.73 (0.14)
200	300	4	0.00 (0.00)	0.02 (0.01)	24.53 (3.18)	1.00 (0.00)	1.00 (0.00)	0.42 (0.12)
200	50	10	0.09 (0.06)	0.22 (0.17)	0.84 (0.92)	0.93 (0.02)	0.91 (0.05)	0.85 (0.13)
200	100	10	0.04 (0.02)	0.17 (0.07)	0.77 (0.24)	0.89 (0.04)	0.92 (0.02)	0.53 (0.12)
200	200	10	0.05 (0.00)	0.14 (0.01)	8.15 (2.22)	0.96 (0.02)	0.67 (0.14)	0.50 (0.14)
400	50	4	0.00 (0.00)	0.00 (0.00)	0.02 (0.00)	0.89 (0.04)	0.89 (0.03)	0.90 (0.03)
400	100	4	0.00 (0.00)	0.00 (0.00)	0.04 (0.00)	0.90 (0.05)	0.90 (0.04)	0.96 (0.03)
400	200	4	0.00 (0.00)	0.00 (0.00)	0.05 (0.01)	1.00 (0.00)	1.00 (0.00)	1.00 (0.00)
400	50	10	0.02 (0.02)	0.05 (0.03)	0.26 (0.16)	0.94 (0.02)	0.92 (0.02)	0.94 (0.03)
400	100	10	0.02 (0.02)	0.04 (0.02)	0.38 (0.34)	0.94 (0.02)	0.94 (0.02)	0.93 (0.04)

Table 1: For the HS-DPM, NG-DPM, and N-DPM models, mean (standard error) of predictive accuracy, variable selection accuracy, and clustering accuracy statistics, obtained over 10 replications, for each of the simulation conditions. Best performance values are indicated in bold.

The results of the simulation study are as follows. As shown in Table 1, the HS-DPM and NG-DPM models generally outperformed the N-DPM in terms of predictive criteria and coefficient estimation under most of the conditions defined by n , p and J . The HS-DPM model emerged as the winner in most of the simulation scenarios. For example, under the

setting of $n = 200$ and $J = 4$, for low dimensional cases ($p = 10$ or 50), all three DPM models perform comparatively in prediction, coefficient estimation and variable selection accuracy. While under moderate to high dimensional scenarios ($p = 200$ or 300), the HS-DPM and NG-DPM models had significantly better predictive and variable selection performances according to the $L1$, $L2$, ASE and A-AUC score, thanks to the effect of Horseshoe or Normal-Gamma prior which can provide better coefficient estimations by adaptively shrinking the coefficients of irrelevant covariates towards zero. In terms of clustering accuracy, all three models perform competitively well due to the nature of joint modeling on the covariates and response, which is usually dominated by the similarity among covariate values when p is not small.

4 Real Data Illustration

We also illustrate our proposed HS-DPM and NG-DPM models through the analysis of the Tehran Residential Building data set (Rafiei and Adeli, 2016), obtained from the UCI Machine Learning repository. The data set contains 372 single-family residential buildings in Tehran, Iran, during 1993 through 2008, each building having between 3 to 9 stories. The data set contains corresponding observations of 9 project physical and financial variables, including total floor area (V1), lot area (V2), total preliminary estimated construction cost (V3), preliminary estimated construction cost (V4), equivalent preliminary estimated construction cost in base year (V5), duration of construction (V6), unit price at project beginning (V7), sales price, and construction cost. The data set also includes corresponding observations of 19 economic variables in 5 time-lag numbers before the initial construction date of the building; and observations of the variable named profit, defined by the difference of sales price and construction cost of the building project.

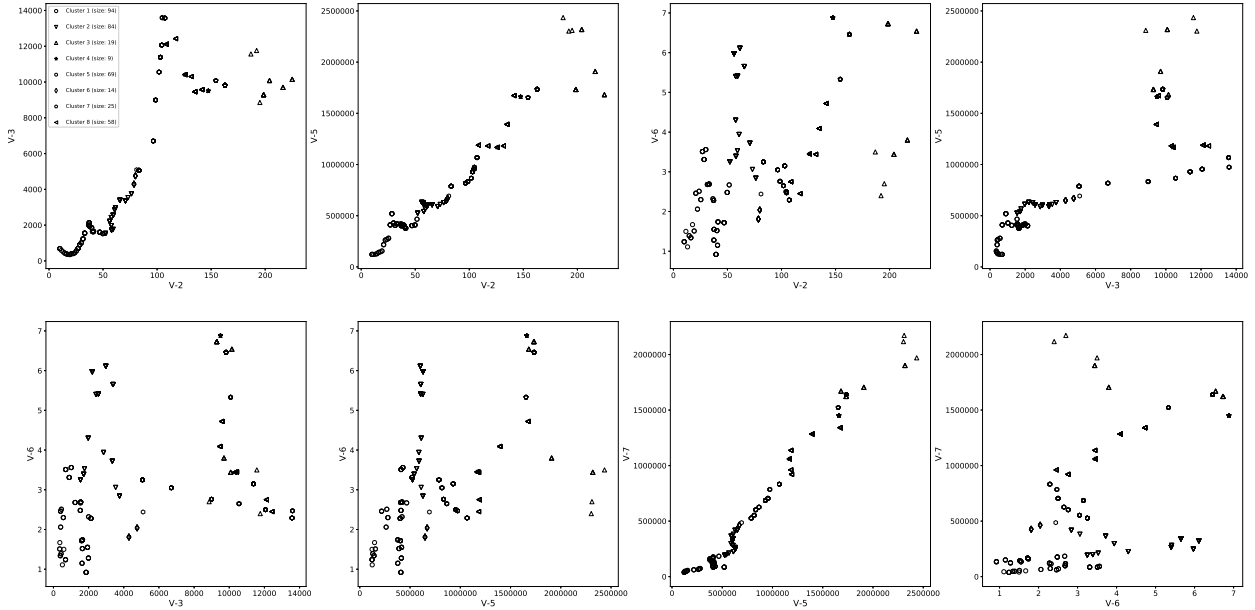


Figure 1: For the HS-DPM model, the clustering estimate, according to 2-dimensional views of covariate observations.

The aim of the data analysis was to predict log profit of the construction project as a function of 102 covariates, including the physical or financial variables (V1 to V7) and all the 95 economic variables ($7 + 19(5) = 102$). Also, the aim was to estimate the latent clustering groups of the building projects, and to identify the subsets of relevant (and irrelevant) covariates of profit, for each cluster.

The HS-DPM, NG-DPM, and the benchmark N-DPM models were each fitted to the residential data set, using the same prior (except for mass parameter α) and MCMC specifications used in Section 3. As another benchmark model, we also analyzed the data using the Bayesian Horseshoe (HS) normal linear regression model from R code with default prior specifications in Gramacy (2019), while this model does not perform clustering. The predictive performances of all four models were also evaluated by the mean of $L1$ and $L2$ prediction error, measured through 5-fold cross validation, based on a train-test split ratio of 0.2. For each fold of splitting, we normalized the training data observations of each variable into z -scores having mean 0 and variance 1, and then fit the transformation on the test data accordingly.

Both the HS-DPM and NG-DPM models significantly outperformed the benchmark N-DPM model in terms of predictive accuracy, apparently because of more accurate coefficient estimation under the cluster-wise "high-dimensional"

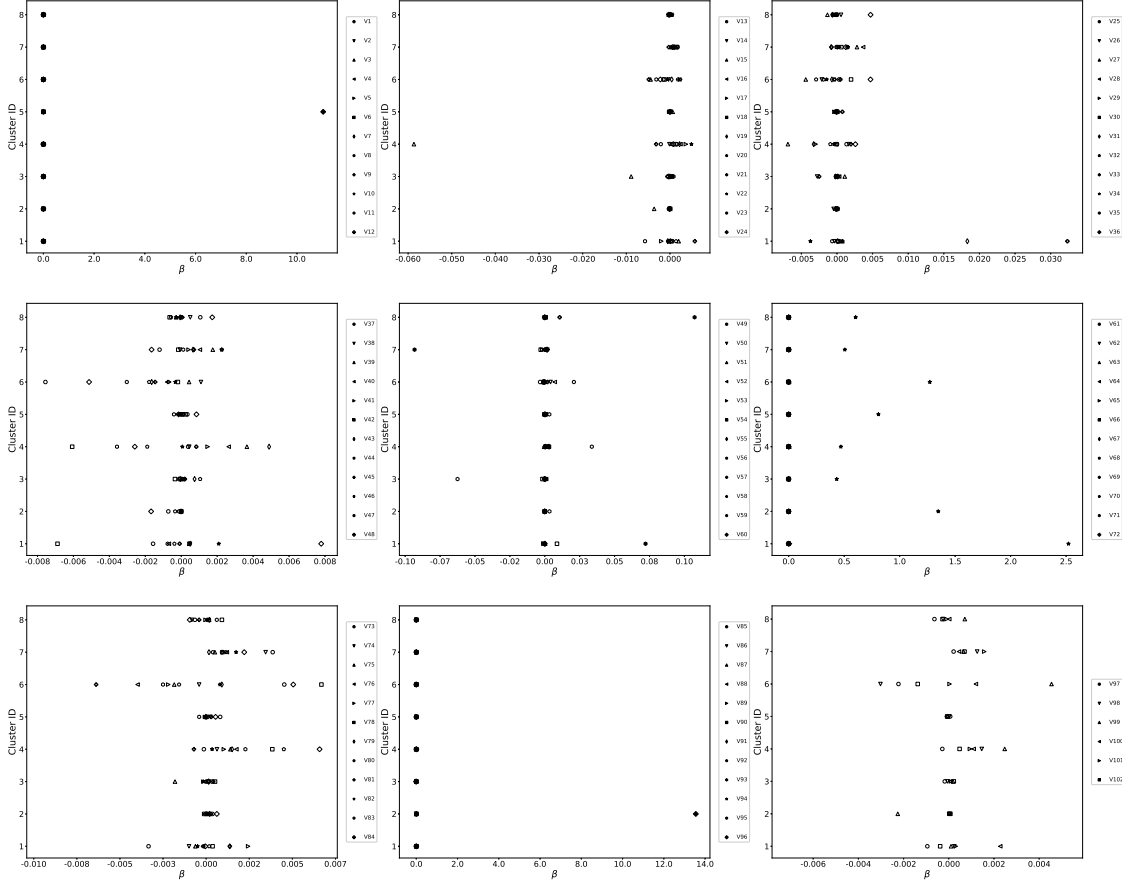


Figure 2: For the HS-DPM model, the marginal posterior medians of all 102 regression coefficients, and cluster-wise variable selection results. A filled marker indicates a significant covariate according to the SN criterion using threshold $p^* = 0.5$.

scenarios. The (mean $L2$) prediction errors for the models were, respectively, HS-DPM (0.08), NG-DPM (0.27), HS (0.28), and N-DPM (0.89); while the four models were similarly ordered with respect to mean $L1$ prediction error. For the predictive comparison between our proposed models and HS, the HS-DPM model was still the obvious winner, while HS and NG-DPM performed comparatively.

In addition, we inspected the respective clustering estimates of the HS-DPM, NG-DPM, and N-DPM models, obtained from the entire data set. Clustering solutions are similar for three models, each of which estimated 8 clusters from the data, due to the same prior specification on the mass parameter and the joint DPM clustering rule. The estimated clustering for the HS-DPM model, along with corresponding cluster size, is presented in Figure 1, which leads to useful interpretations. For example, as the largest group, Cluster 1 generally displays construction projects with small lot area and low construction cost, and is one of the largest cluster groups. In contrast, the building projects allocated into the third cluster group tend to have larger lot area and higher construction costs.

Figure 2 presents the cluster-wise variable selection results for the HS-DPM model, indicating which variables were relevant or irrelevant in the prediction of log profit. While most of the regression coefficients estimations were similar across different clusters, some coefficient estimations and sparsity patterns differed across the cluster groups, with V70 (total floor areas of building permits issued by city in 4th time lag) as a relevant covariate for prediction for all cluster groups.

5 Conclusions

We proposed two novel joint DPM models, namely the HS-DPM and the NG-DPM, each of which adopt a continuous shrinkage (baseline) prior on the regression coefficients, to provide flexible prediction and cluster-wise variable

selection. The development of these models was motivated by the fact that most of the existing literature either focuses on the standard benchmark DPM model, which adopts a conjugate non-shrinkage normal baseline prior on regression coefficients which allows for easier posterior computations, but does not allow for heterogeneous variable selections across different cluster groups; or focuses on the spike-and-slab baseline prior for covariate selection based on latent binary variables, which is computationally costly when the number of covariates is large.

Our models were able to provide inference on variable selection, while maintaining a computational cost comparable with that of the standard benchmark DPM model. In the simulation study, we have shown that the HS-DPM and the NG-DPM models generally provided better prediction, coefficient estimation, and cluster-wise variable selection accuracy than the benchmark model, especially when number of covariates is much larger than the within-cluster sample size. We also highlighted the advantage in prediction for our proposed models, and presented corresponding clustering and cluster-wise variable selection idea through a real data application. The improvement in prediction compared with the Bayesian Horseshoe normal linear model was also presented to show the benefits of allowing for heterogeneous sparsity patterns across different clusters of the data set.

For future research, the novel models can be extended to mixtures of generalized linear models in order to address additional types of dependent response variables, such as binary response. The models can also be extended to other types nonparametric priors which generalize the DP to offer more flexibility in the analysis of the relationship between covariates and response.

Acknowledgments

The article represents work from the first author’s Ph.D. dissertation, and is supported by National Science Foundation grant SES-1156372 awarded to the second author.

References

- Andrews, D. F. and C. L. Mallows (1974). Scale mixtures of normal distributions. *Journal of the Royal Statistical Society, Series B* 36, 99–102.
- Barcella, W., M. De Iorio, and G. Baio (2017). A comparative review of variable selection techniques for covariate dependent Dirichlet process mixture models. *Canadian Journal of Statistics* 45, 254–273.
- Barcella, W., M. De Iorio, G. Baio, and J. Malone-Lee (2016). Variable selection in covariate dependent random partition models: An application to urinary tract infection. *Statistics in Medicine* 35, 1373–1389.
- Carvalho, C. M., N. G. Polson, and J. G. Scott (2009). Handling sparsity via the horseshoe. *Journal of Machine Learning Research W&CP* 5, 73–80.
- Carvalho, C. M., N. G. Polson, and J. G. Scott (2010). The horseshoe estimator for sparse signals. *Biometrika* 97, 465–480.
- Castillo, I., J. Schmidt-Hieber, and A. Van der Vaart (2015). Bayesian linear regression with sparse priors. *Annals of Statistics* 43, 1986–2018.
- Escobar, M. D. (1994). Estimating normal means with a Dirichlet process prior. *Journal of the American Statistical Association* 89, 268–277.
- Escobar, M. D. and M. West (1995). Bayesian density estimation and inference using mixtures. *Journal of the American Statistical Association* 90, 577–588.
- Ferguson, T. S. (1973). A Bayesian analysis of some nonparametric problems. *Annals of Statistics* 1, 209–230.
- Gramacy, R. B. (2019). Package ‘monomvn’. *R package version*, 1–9.
- Griffin, J. E. and P. J. Brown (2010). Inference with normal-gamma prior distributions in regression problems. *Bayesian Analysis* 5, 171–188.
- Hannah, L. A., D. M. Blei, and W. B. Powell (2011). Dirichlet process mixtures of generalized linear models. *Journal of Machine Learning Research* 12, 1923–1953.
- Hubert, L. and P. Arabie (1985). Comparing partitions. *Journal of Classification* 2, 193–218.
- Karabatsos, G. and S. G. Walker (2012). Bayesian nonparametric mixed random utility models. *Computational Statistics & Data Analysis* 56, 1714–1722.
- Li, Q. and N. Lin (2010). The Bayesian elastic net. *Bayesian Analysis* 5, 151–170.

- MacEachern, S. N. (1999). Dependent nonparametric processes. In *ASA Proceedings of the Section on Bayesian Statistical Science*, Volume 1, pp. 50–55. Alexandria, Virginia. Virginia: American Statistical Association; 1999.
- Makalic, E. and D. F. Schmidt (2015). A simple sampler for the horseshoe estimator. *IEEE Signal Processing Letters* 23, 179–182.
- Meilă, M. (2007). Comparing clusterings—an information based distance. *Journal of Multivariate Analysis* 98, 873–895.
- Neal, R. M. (2003). Slice sampling. *Annals of Statistics* 31, 705–741.
- Park, T. and G. Casella (2008). The Bayesian Lasso. *Journal of the American Statistical Association* 103, 681–686.
- Quintana, F. A., P. Müller, A. Jara, and S. N. MacEachern (2020). The dependent Dirichlet process and related models. *arXiv preprint arXiv:2007.06129*.
- Quintana, F. A., P. Müller, and A. L. Papoila (2015). Cluster-specific variable selection for product partition models. *Scandinavian Journal of Statistics* 42, 1065–1077.
- Rafiei, M. H. and H. Adeli (2016). A novel machine learning model for estimation of sale prices of real estate units. *Journal of Construction Engineering and Management* 142, 04015066.
- Rastelli, R. and N. Friel (2018). Optimal Bayesian estimators for latent variable cluster models. *Statistics and Computing* 28, 1169–1186.
- Sethuraman, J. (1994). A constructive definition of Dirichlet priors. *Statistica Sinica* 4, 639–650.
- Tibshirani, R. (1996). Regression shrinkage and selection via the lasso. *Journal of the Royal Statistical Society, Series B* 58, 267–288.
- Tibshirani, R. (2011). Regression shrinkage and selection via the lasso: A retrospective. *Journal of the Royal Statistical Society, Series B* 73, 273–282.
- Wade, S., D. B. Dunson, S. Petrone, and L. Trippa (2014). Improving prediction from Dirichlet process mixtures via enrichment. *Journal of Machine Learning Research* 15, 1041–1071.

A MCMC Algorithm for the HS-DPM Model

Equation (5) gives the joint posterior distribution of the model parameters, up to a proportionality constant. Based on the "scale mixture" relationship between half-Cauchy distribution and Inverse-Gamma distribution (Makalic and Schmidt, 2015), we can rewrite model (3) by augmentation of hyperparameters as:

$$\mathbf{\Gamma}_j = \text{diag}(\gamma_{j1}^2, \dots, \gamma_{jp}^2) \equiv \text{diag}(\gamma_j^2), \quad j = 1, 2, \dots \quad (7a)$$

$$\pi(\gamma_j^2 | \nu_j) = \prod_{l=1}^p IG(\gamma_{jl}^2 | 1/2, 1/\nu_{jl}), \quad j = 1, 2, \dots \quad (7b)$$

$$\pi(\zeta_j^2 | \xi_j) = IG(\zeta_j^2 | 1/2, 1/\xi_j), \quad j = 1, 2, \dots \quad (7c)$$

$$\pi(\nu_{1j}, \dots, \nu_{pj}, \xi_j) = \prod_{l=1}^p IG(\nu_{jl} | 1/2, 1) IG(\xi_j | 1/2, 1), \quad j = 1, 2, \dots \quad (7d)$$

Then the MCMC algorithm for sampling the posterior distributions from HS-DPM model is described as follows:

Step 0: Initialization: Denote s as the iteration index within MCMC algorithm. Initialize with starting values by setting $s = 0$, draw $d_i^{(0)} \sim \text{DiscreteUniform}(1, n)$ for $i = 1, \dots, n$, and $\sigma^{2(0)} \sim IG(\alpha_0, \theta_0)$. Then for $j = 1, \dots, M^{(0)} = \max_i d_i^{(0)}$, $\nu_{jl}^{(0)} \sim IG(1/2, 1)$, $\xi_j^{(0)} \sim IG(1/2, 1)$, $\gamma_{jl}^{2(0)} \sim IG(1/2, 1/\nu_{jl}^{(0)})$, $\zeta_j^{2(0)} \sim IG(1/2, 1/\xi_j^{(0)})$.

We also initialize starting values for $\mu_j^{(0)} \sim \mathcal{N}(0, \nu_\mu)$, $\beta_j^{(0)} \sim \mathcal{N}(\mathbf{0}_p, \zeta_j^{2(0)} \sigma^{2(0)} \mathbf{\Gamma}_j^{(0)})$, $m_{jl}^{(0)} \sim \mathcal{N}(m_0, \tau_{jl}^{(0)}/n_0)$, $\tau_{jl}^{(0)} \sim IG(\frac{\nu_0}{2}, \frac{2}{\nu_0 s_0^2})$, and mass parameter $\alpha^{(0)} \sim Ga(\alpha_\alpha, \theta_\alpha)$.

Then, for each iteration $s = 1, \dots, S$, draw from the full conditional posterior distributions described in the following steps:

Step 1: Draw mixture weights $w_j^{(s)}$: For $j = 1, \dots, M^{(s)} = \max_i d_i^{(s-1)}$, take $n_j^{(s)} = \sum_{i=1}^n \mathbf{1}(d_i^{(s-1)} = j)$, $m_j^{(s)} = \sum_{i=1}^n \mathbf{1}(d_i^{(s-1)} > j)$. Then for $j = 1, \dots, M^{(s)}$, draw $v_j^{(s)} \sim \text{Beta}(1+n_j^{(s)}, \alpha^{(s-1)}+m_j^{(s)})$, let $w_j^{(s)} = v_j^{(s)} \prod_{l < j} (1-v_l^{(s)})$,

and draw $u_i^{(s)} \sim \text{Unif}(0, w_{d_i^{(s-1)}}^{(s)})$ for $i = 1, \dots, n$, where $\text{Unif}(c, d)$ is the Uniform distribution with parameters c and d . For $j = M^{(s)} + 1, \dots, N^{(s)}$, draw $v_j^{(s)} \sim \text{Beta}(1 + n_j^{(s)}, \alpha^{(s-1)} + m_j^{(s)})$ until the smallest $N^{(s)}$ is obtained such that $\sum_{j=1}^{N^{(s)}} w_j^{(s)} > \max_i(1 - u_i^{(s)})$.

Step 2: For $j = 1, \dots, M^{(s)}$, update $\nu_j^{(s)}, \xi_j^{(s)}, \gamma_j^{2(s)}, \zeta_j^{2(s)}, \mu_j^{(s)}, \beta_j^{(s)}, \mathbf{m}_j^{(s)}, \tau_j^{(s)}$:

2.1: For $l = 1, \dots, p$, draw from:

$$\nu_{jl}^{(s)} | \gamma_{jl}^{2(s-1)} \propto \pi(\nu_{jl}) \pi(\gamma_{jl}^{2(s-1)} | \nu_{jl}) \sim \text{IG}(1, 1 + \frac{1}{\gamma_{jl}^{2(s-1)}}).$$

2.2: Draw from:

$$\xi_j^{(s)} | \zeta_j^{2(s-1)} \propto \pi(\xi_j) \pi(\zeta_j^{2(s-1)} | \xi_j) \sim \text{IG}(1, 1 + \frac{1}{\zeta_j^{2(s-1)}}).$$

2.3: For $l = 1, \dots, p$, draw from:

$$\gamma_{jl}^{2(s)} | \nu_{jl}^{(s)}, \zeta_j^{2(s-1)}, \beta_{jl}^{(s-1)}, \sigma^{2(s-1)} \propto \pi(\gamma_{jl}^2 | \nu_{jl}^{(s)}) \pi(\beta_{jl}^{(s-1)} | \gamma_{jl}^2) \sim \text{IG}(1, \frac{1}{\nu_{jl}^{(s)}} + \frac{\beta_{jl}^{(s-1)2}}{2\zeta_j^{2(s-1)}\sigma^{2(s-1)}}).$$

2.4: Draw from:

$$\zeta_j^{2(s)} | \xi_j^{(s)}, \gamma_{jl}^{2(s)}, \beta_{jl}^{(s-1)}, \sigma^{2(s-1)} \propto \pi(\zeta_j^2 | \xi_j^{(s)}) \pi(\beta^{(s-1)} | \zeta_j^2) \sim \text{IG}(\frac{p+1}{2}, \frac{1}{\xi_j^{(s)}} + \sum_{l=1}^p \frac{\beta_{jl}^{2(s-1)}}{\gamma_{jl}^{2(s)}}).$$

2.5: Draw from:

$$\begin{aligned} \mu_j^{(s)}, \beta_j^{(s)} | \gamma_{jl}^{2(s)}, \zeta_j^{2(s)}, \sigma^{2(s-1)} &\propto \prod_{d_i^{(s-1)}=j} \mathcal{N}(y_i | \mathbf{x}_i, \mu_j, \beta_j, \sigma^{2(s-1)}) \pi(\beta_j | \gamma_{jl}^{2(s)}, \zeta_j^{2(s)}, \sigma^{2(s-1)}) \pi(\mu_j) \\ &\sim \mathcal{N}_{p+1}(B^{-1} \tilde{\mathbf{X}}_j^{*T} \mathbf{y}_j^*, \sigma^{2(s-1)} B^{-1}), \end{aligned}$$

where $B = \tilde{\mathbf{X}}_j^{*T} \tilde{\mathbf{X}}_j^* + \sigma^{2(s-1)} \mathbf{\Gamma}_j^{*(s)}$, $\tilde{\mathbf{X}}_j^{*T} = [\mathbf{1}_{n_j}, \mathbf{X}_j^*]$, $\mathbf{\Gamma}_j^{*(s)} = \frac{1}{\zeta_j^{2(s)}} \text{diag}(0, 1/\gamma_{j1}^{2(s)}, \dots, 1/\gamma_{jp}^{2(s)})$.

2.6: For $l = 1, \dots, p$, draw from:

$$\tau_{jl}^{(s)} \propto \prod_{d_i^{(s-1)}=j} \mathcal{N}(x_{il} | m_{jl}^{(s-1)}, \tau_{jl}) \pi(\tau_{jl}) \sim \text{IG}(\frac{\nu^*}{2}, \frac{2}{s^* 2\nu^*}),$$

where $n^* = n_0 + n_j$, $\nu^* = \nu_0 + n_j$, $\bar{x}_{n_j, l} = \frac{1}{n_j} \sum_{i=1}^{n_j} x_{il}$, and $s^{*2} = \frac{1}{\nu^*} \left[\sum_{i=1}^{n_j} (x_{il} - \bar{x}_{n_j, l})^2 + s_0^2 \nu_0 + \frac{n_0 n_j}{n^*} (\bar{x}_{n_j, l} - m_0)^2 \right]$.

2.7: For $l = 1, \dots, p$, draw from:

$$m_{jl}^{(s)} | \tau_{jl}^{(s)} \propto \prod_{d_i^{(s-1)}=j} \mathcal{N}(x_{il} | m_{jl}, \tau_{jl}^{(s)}) \pi(m_{jl} | \tau_{jl}^{(s)}) \sim \mathcal{N}(m^*, \frac{\tau_{jl}^{(s)}}{n^*}),$$

where $m^* = (n_j \bar{x}_{n_j, l} + n_0 m_0) / (n_j + n_0)$.

If $N^{(s)} > M^{(s)}$, then for $j = M^{(s)} + 1, \dots, N^{(s)}$, draw $\nu_{jl}^{(s)} \sim \text{IG}(1/2, 1)$, $\xi_j^{(s)} \sim \text{IG}(1/2, 1)$, $\gamma_{jl}^{2(s)} \sim \text{IG}(1/2, 1/\nu_{jl}^{(s)})$, $\zeta_j^{2(s)} \sim \text{IG}(1/2, 1/\xi_j^{(s)})$, $\mu_j^{(s)} \sim \mathcal{N}(0, \nu_\mu)$, $\beta_j^{(s)} \sim \mathcal{N}_p(\mathbf{0}_p, \zeta_j^{2(s)} \sigma^{2(s-1)} \mathbf{\Gamma}_j^{(s)})$, $m_{jl}^{(s)} \sim \mathcal{N}(m_0, \tau_{jl}^{(s)}/n_0)$, $\tau_{jl}^{(s)} \sim \text{IG}(\frac{\nu_0}{2}, \frac{2}{\nu_0 s_0^2})$,

Step 3: For $i = 1, \dots, n$, sample $d_i^{(s)} = j$ with probability proportional to:

$$\mathbf{1}(w_j^{(s)} > u_i^{(s)}) \mathcal{N}(y_i | \mu_j^{(s)} + \mathbf{x}_i^T \boldsymbol{\beta}_j^{(s)}, \sigma^{2(s-1)}) \mathcal{N}_p(\mathbf{x}_i | \mathbf{m}_j^{(s)}, \boldsymbol{\tau}_j^{(s)}), \text{ for } j = 1, \dots, N^{(s)}.$$

Step 4: Once we obtain $d_i^{(s)}$ for $i = 1, \dots, n$, we have the distinct set of coefficients $\{\boldsymbol{\beta}_1^{*(s)}, \dots, \boldsymbol{\beta}_K^{*(s)}\}$ among $\{\boldsymbol{\beta}_{d_i}^{(s)}\}$, and corresponding distinct sets $\{\gamma_1^{*2(s)}, \dots, \gamma_K^{*2(s)}\}$ and $\{\xi_1^{*2(s)}, \dots, \xi_K^{*2(s)}\}$, where K is number of unique $d_i^{(s)}$'s. Then draw from:

$$\begin{aligned} \sigma^{2(s)} | \boldsymbol{\beta}_k^*, \mu_k^* &\propto \prod_{i=1}^n \mathcal{N}(y_i | \mu_{d_i}^{(s)} + \mathbf{x}_i^T \boldsymbol{\beta}_{d_i}^{(s)}, \sigma^2) \pi(\sigma^2) \pi(\boldsymbol{\beta}) \\ &\sim IG\left((n+p)/2 + \alpha_0, \sum_{i=1}^n (y_i - \mu_{d_i}^{(s)} - \mathbf{x}_i^T \boldsymbol{\beta}_{d_i}^{(s)})^2 / 2 + \sum_{k=1}^K \frac{1}{2\xi_k^{*2(s)}} \sum_{l=1}^p \frac{\beta_{lk}^{*2(s)}}{\gamma_{lk}^{*2(s)}} + \theta_0\right). \end{aligned}$$

Step 5: Update $\alpha^{(s)}$ by drawing from a Gamma distribution with shape $\alpha_\alpha + K - \mathbf{1}(u > \{O/(1+O)\})$ and scale $\theta_\alpha - \log(\eta)$, where $\eta \sim \text{Beta}(\alpha^{(s-1)} + 1, n)$, $u \sim \text{Unif}(0, 1)$ and $O = (\alpha_\alpha + K - 1) / (\{\theta_\alpha - \log(\eta)\}n)$ (Escobar and West, 1995).

Sampling updates from Steps 1 through 5 are repeated for a large number of iterations until the MCMC chain has displayed good mixing, according to trace plots.

B MCMC Algorithm for the NG-DPM Model

The MCMC algorithm for sampling the posterior distributions from NG-DPM model is described as follows:

Step 0: Initialization: Denote s as the iteration index within MCMC algorithm. Initialize with starting values by setting $s = 0$, draw $d_i^{(0)} \sim \text{DiscreteUniform}(1, n)$ for $i = 1, \dots, n$. Then for $j = 1, \dots, M^{(0)} = \max_i d_i^{(0)}$, draw $\lambda_j^{(0)} \sim \text{Exp}(1)$, $\gamma_j^{-2(0)} \sim \text{Ga}(2, \frac{2V}{\lambda_j^{(0)}})$, where $V = \frac{1}{p} \sum_{l=1}^p \hat{\beta}_l^2 \mathbf{1}(n \geq p+1) + \frac{1}{n} \sum_{l=1}^p \tilde{\beta}_l^2 \mathbf{1}(n < p+1)$. We also initialize starting values for $\psi_{jl}^{(0)} \sim \text{Ga}(\lambda_j^{(0)}, 2\gamma_j^{-2(0)})$, $\mu_j^{(0)} \sim \mathcal{N}(0, \nu_\mu)$, $\boldsymbol{\beta}_j^{(0)} \sim \mathcal{N}_p(\mathbf{0}_p, \mathbf{D}_{\psi,j}^{(0)})$, $m_{jl}^{(0)} \sim \mathcal{N}(m_0, \tau_{jl}^{(0)}/n_0)$, $\tau_{jl}^{(0)} \sim \text{IG}(\frac{\nu_0}{2}, \frac{2}{\nu_0 s_0^2})$, $\sigma^{2(0)} \sim \text{IG}(\alpha_0, \theta_0)$, and mass parameter $\alpha^{(0)} \sim \text{Ga}(\alpha_\alpha, \theta_\alpha)$.

Then, for each iteration $s = 1, \dots, S$, draw from the full conditional posterior distributions described in the following steps:

Step 1: Draw mixture weights $w_j^{(s)}$: For $j = 1, \dots, M^{(s)} = \max_i d_i^{(s-1)}$, take $n_j^{(s)} = \sum_{i=1}^n \mathbf{1}(d_i^{(s-1)} = j)$, $m_j^{(s)} = \sum_{i=1}^n \mathbf{1}(d_i^{(s-1)} > j)$. Then for $j = 1, \dots, M^{(s)}$, draw $v_j^{(s)} \sim \text{Beta}(1+n_j^{(s)}, \alpha^{(s-1)} + m_j^{(s)})$, let $w_j^{(s)} = v_j^{(s)} \prod_{l < j} (1 - v_l^{(s)})$, and draw $u_i^{(s)} \sim \text{Unif}(0, w_{d_i^{(s-1)}}^{(s)})$ for $i = 1, \dots, n$. For $j = M^{(s)} + 1, \dots, N^{(s)}$, draw $v_j^{(s)} \sim \text{Beta}(1+n_j^{(s)}, \alpha^{(s-1)} + m_j^{(s)})$ until the smallest $N^{(s)}$ is obtained such that $\sum_{j=1}^{N^{(s)}} w_j^{(s)} > \max_i (1 - u_i^{(s)})$.

Step 2: For $j = 1, \dots, M^{(s)}$, update $\lambda_j^{(s)}$, $\gamma_j^{-2(s)}$, $\boldsymbol{\psi}_j^{(s)}$, $\mu_j^{(s)}$, $\boldsymbol{\beta}_j^{(s)}$, $\mathbf{m}_j^{(s)}$, $\boldsymbol{\tau}_j^{(s)}$:

2.1: Draw from:

$$\lambda_j^{(s)} | \boldsymbol{\psi}_j^{(s-1)}, \gamma_j^{-2(s-1)} \propto \pi(\lambda_j) \prod_{l=1}^p \pi(\psi_{jl}^{(s-1)} | \lambda_j, \gamma_j^{-2(s-1)}) \propto \pi(\lambda_j) \left(\frac{1}{2} \gamma_j^{-2(s-1)}\right)^{p\lambda_j} [\Gamma(\lambda_j)]^{-p} \left[\prod_{l=1}^p \psi_{jl}^{(s-1)}\right]^{\lambda_j}.$$

Since the conditional posterior distribution is not in closed form, we perform a sampling update of λ_j using the stepping-out slice sampling algorithm (Neal, 2003).

2.2: Draw from:

$$\begin{aligned} \gamma_j^{-2(s)} |\lambda_j^{(s)}, \psi_j^{(s-1)} &\propto \pi(\gamma_j^{-2} |\lambda_j^{(s)}) \prod_{l=1}^p \pi(\psi_{jl}^{(s-1)} | \lambda_j^{(s)}, \gamma_j^{-2}) \propto Ga(\gamma_j^{-2} | 2, V/2\lambda_j^{(s)}) \prod_{l=1}^p \left[(2\gamma_j^{-2})^\lambda \exp\left\{-\frac{1}{2}\gamma_j^{-2}\psi_{jl}^{(s-1)}\right\} \right] \\ &\sim Ga\left(p\lambda_j^{(s)} + 2, \left[\frac{1}{2} \sum_{l=1}^p \psi_{jl}^{(s-1)} + V/2\lambda_j^{(s)}\right]\right). \end{aligned}$$

2.3: For $l = 1, \dots, p$, draw from the Generalized Inverse Gaussian (*GIG*) distribution, where $GIG(c, d, h)$ has the probability density

$$f(x) = \frac{(c/d)^{h/2}}{2K_h(\sqrt{cd})} x^{h-1} e^{(cx+d/x)/2}.$$

$$\begin{aligned} \psi_{jl}^{(s)} | \beta_{jl}^{(s-1)}, \lambda_j^{(s)}, \gamma_j^{-2(s)} &\propto \pi(\psi_{jl} | \lambda_j^{(s)}, \gamma_j^{-2(s)}) \pi(\beta_{jl}^{(s-1)} | \psi_{jl}) \propto \psi_{jl}^{\lambda_j^{(s)} - 1} \exp\left\{-\frac{1}{2}\gamma_j^{-2(s)}\psi_{jl}\right\} \psi_{jl}^{-\frac{1}{2}} \exp\left\{-\frac{1}{2\psi_{jl}}\beta_{jl}^{2(s-1)}\right\} \\ &\sim GIG\left(\lambda_j^{(s)} - \frac{1}{2}, \gamma_j^{-2(s)}, \beta_{jl}^{2(s-1)}\right). \end{aligned}$$

2.4: If $n_j > p + 1$, draw from:

$$\begin{aligned} \mu_j^{(s)}, \beta_j^{(s)} | \mathbf{D}_{\psi, j}^{(s)}, \sigma^{2(s-1)} &\propto \prod_{d_i^{(s-1)}=j} \mathcal{N}(y_i | \mathbf{x}_i, \mu_j, \beta_j, \sigma^{2(s-1)}) \pi(\beta_j | \mathbf{D}_{\psi, j}^{(s)}) \pi(\mu_j) \\ &\sim \mathcal{N}_{p+1}(B^{-1} \tilde{\mathbf{X}}_j^{*T} \mathbf{y}_j^*, \sigma^{2(s-1)} B^{-1}), \end{aligned}$$

where $B = \tilde{\mathbf{X}}_j^{*T} \tilde{\mathbf{X}}_j^* + \sigma^{2(s-1)} \Lambda_j^{(s)}$, $\tilde{\mathbf{X}}_j^{*T} = [\mathbf{1}_{n_j}, \mathbf{X}_j^*]$, $\Lambda_j^{(s)} = \text{diag}\left(0, 1/\psi_{j1}^{(s)}, \dots, 1/\psi_{jp}^{(s)}\right)$. Otherwise, if $n_j \leq p + 1$, we take the singular value decomposition $\tilde{\mathbf{X}}_j^* = F^T D A^T$, and let $\hat{\theta}_{n_j} = D^{-1} F \mathbf{y}_j^*$. Then we draw from:

$$\mu_j^{(s)}, \beta_j^{(s)} | \mathbf{D}_{\psi, j}^{(s)}, \sigma^{2(s-1)} \sim \mathcal{N}_{p+1}(\Psi_j^{(s)} A C^{-1} \hat{\theta}_{n_j}, \Psi_j^{(s)} - \Psi_j^{(s)} A C^{-1} A^T \Psi_j^{(s)})$$

where $\Psi_j^{(s)} = \text{diag}\left(\nu_\mu, \psi_{j1}^{(s)}, \dots, \psi_{jp}^{(s)}\right)$, $C = \Psi_{0j} + \sigma^{2(s-1)} \Lambda^*$, $\Psi_{0j} = A^T \Psi_j^{(s)} A$, $\Lambda^* = D^{-2}$.

2.5: For $l = 1, \dots, p$, draw from:

$$\tau_{jl}^{(s)} \propto \prod_{d_i^{(s-1)}=j} \mathcal{N}(x_{il} | m_{jl}^{(s-1)}, \tau_{jl}) \pi(\tau_{jl}) \sim IG\left(\frac{\nu^*}{2}, \frac{2}{s^* 2 \nu^*}\right),$$

where $n^* = n_0 + n_j$, $\nu^* = \nu_0 + n_j$, $\bar{x}_{n_j, l} = \frac{1}{n_j} \sum_{i=1}^{n_j} x_{il}$, and $s^* 2 = \frac{1}{\nu^*} \left[\sum_{i=1}^{n_j} (x_{il} - \bar{x}_{n_j, l})^2 + s_0^2 \nu_0 + \frac{n_0 n_j}{n^*} (\bar{x}_{n_j, l} - m_0)^2 \right]$.

2.6: For $l = 1, \dots, p$, draw from:

$$m_{jl}^{(s)} | \tau_{jl}^{(s)} \propto \prod_{d_i^{(s-1)}=j} \mathcal{N}(x_{il} | m_{jl}, \tau_{jl}^{(s)}) \pi(m_{jl} | \tau_{jl}^{(s)}) \sim \mathcal{N}\left(m^*, \frac{\tau_{jl}^{(s)}}{n^*}\right),$$

where $m^* = (n_j \bar{x}_{n_j, l} + n_0 m_0) / (n_j + n_0)$.

If $N^{(s)} > M^{(s)}$, then for $j = M^{(s)} + 1, \dots, N^{(s)}$, draw $\lambda_j^{(s)} \sim \text{Exp}(1)$, $\gamma_j^{-2(s)} \sim Ga(2, V/2\lambda_j^{(s)})$, $\psi_j^{(s)} \sim \prod_{l=1}^p Ga(\lambda_j^{(s)}, \gamma_j^{-2(s)})$, $\beta_j^{(s)} \sim \mathcal{N}(\mathbf{0}_p, \mathbf{D}_{\psi, j}^{(s)})$, $\mu_j^{(s)} \sim \mathcal{N}(0, \nu_\mu)$, $\tau_j^{(s)} \sim \prod_{l=1}^p IG(\nu_0/2, 2/\nu_0 s_0^2)$, $\mathbf{m}_j^{(s)} \sim \prod_{l=1}^p \mathcal{N}(m_0, \tau_{jl}^{(s)}/n_0)$.

Step 3: For $i = 1, \dots, n$, sample $d_i^{(s)} = j$ with probability proportional to:

$$\mathbf{1}(w_j^{(s)} > u_i^{(s)}) \mathcal{N}(y_i | \mu_j^{(s)} + \mathbf{x}_i^T \beta_j^{(s)}, \sigma^{2(s-1)}) \mathcal{N}_p(\mathbf{x}_i | \mathbf{m}_j^{(s)}, \tau_j^{(s)}), \text{ for } j = 1, \dots, N^{(s)}.$$

Step 4: Draw from:

$$\begin{aligned} \sigma^{2(s)} | \beta_k^*, \mu_k^* &\propto \prod_{i=1}^n \mathcal{N}(y_i | \mu_{d_i}^{(s)} + \mathbf{x}_i^T \beta_{d_i}^{(s)}, \sigma^2) \pi(\sigma^2) \\ &\sim IG\left(n/2 + \alpha_0, \sum_{i=1}^n (y_i - \mu_{d_i}^{(s)} - \mathbf{x}_i^T \beta_{d_i}^{(s)})^2 / 2 + \theta_0\right). \end{aligned}$$

Step 5: Update $\alpha^{(s)}$ by drawing from a Gamma distribution with shape $\alpha_\alpha + K - \mathbf{1}(u > \{O/(1+O)\})$ and scale $\theta_\alpha - \log(\eta)$, where K is number of unique $d_i^{(s)}$'s, $\eta \sim \text{Beta}(\alpha^{(s-1)} + 1, n)$, $u \sim \text{Unif}(0, 1)$ and $O = (\alpha_\alpha + K - 1) / (\{\theta_\alpha - \log(\eta)\}n)$ (Escobar and West, 1995).

Sampling updates from Steps 1 through 5 are repeated for a large number of iterations until the MCMC chain has displayed good mixing, according to trace plots.

The Python code and the R code files, provide more details about the MCMC sampling algorithm, along with the MCMC code files for the N-DPM model, and the simulated data sets and real data set analyzed in Sections 3 and 4 of the article.